Eur. Phys. J. D **27**, 231–237 (2003)
DOI: 10.1140/epjd/e2003-00277-3

THE EUROPEAN PHYSICAL JOURNAL D

Thermal evolution of cluster assembled Ni_3Al materials modelled at the atomic scale

P. Moskovkin[1,2] and M. Hou[1,a]

[1] Physique des Solides Irradiés et des Nanostructures, CP234, Université Libre de Bruxelles, boulevard du Triomphe, 1050 Brussels, Belgium
[2] RRC "Kurchatov Institute", Moscow, Russia

Received 21 March 2003 / Received in final form 20 June 2003
Published online 16 September –

Abstract. Diffusion properties of Ni_3Al cluster assembled nanostructured materials are investigated at the atomic scale. Two different model samples are considered, at equilibrium at 300 K. One is obtained by modelling cluster compaction under 2 GPa external pressure and the second by accumulating low energy deposited clusters on a Ni surface. They differ essentially by their density, the latter sample presenting an interconnected network of nanopores, which is not observed in the former. At elevated temperatures, cluster coalescence is observed in both, as well as an intense atomic diffusion at the internal surfaces and nanograin interfaces. A method is presented which allows, in a good approximation, to distinguish between the two phenomena and to estimate diffusion coefficients. At temperatures above 400 K, it is found for both samples, irrespective to their density, that the diffusion activation energy at the internal surfaces and interfaces is as low as in a liquid while the grain cores remain crystalline.

PACS. 61.43.Bn Structural modeling: serial-addition models, computer simulation – 36.40.-c Atomic and molecular clusters – 61.46.+w Nanoscale materials: clusters, nanoparticles, nanotubes, and nanocrystals

1 Introduction

Bi-metallic nanoparticles are at the origin of several technological challenges involving catalytic, optical, magnetic and electronic applications. Isolated particles have properties specific to the nanosize and an important question is to identify to which extent their properties may be retained when assembling them to form a bulk nanostructured material. A corollary question is to identify possible properties of such new materials and this is the frame of the present work. One significant finding in this direction is superplasticity, experimentally evidenced in nanostructured materials [1], which stimulated the question of interfacial state and mechanical deformation. Since one decade, interfacial states and deformation mechanisms are subjected to substantial studies [1–8]. Bulk properties of nanostructured materials depend on the synthesis method and we focus here on systems formed by nanoparticles as building blocks. Starting with nanoparticles, bulk nanostructured materials may be synthethised by assembling them from the gas phase by inert gas condensation followed by compaction or by low energy deposition on a substrate surface. One obvious question is the role of the synthesis itself on the modification of the nanoparticle properties. The capillary pressure in an isolated particle may be quite high and was estimated theoretically of the order of 2 GPa typically, in metallic particles of the order of 2 to 10 nm diameter [9]. A possible consequence in a bi-metallic particle is an enhanced surface segregation of one of the species, as predicted by atomic scale modelling [10]. It comes out modelling that this pressure, induced by the presence of free surfaces is replaced by interfacial stress when the nanoparticles are assembled. The interfacial segregation state is predicted closely similar to that of the isolated clusters [11]. In case of particle deposition modelling shows that the particle-surface interaction may have important consequences, depending upon the deposition energy [12,13] and the nature of the substrate [14,15]. Profound atomic rearrangement is possible in the particle [14,16,17] characterised by a competition between chemical and structural ordering in case of bi-metallic particles [11,15]. Nevertheless, modelling predicts that the structural and thermodynamic properties of the nanoparticles are generally retrieved to a large extent after assembling. As temperature is concerned, it was predicted in [15] that it influences the competition between structural and chemical order at the vicinity of the interface with a substrate during low energy cluster beam deposition. In the present work, we investigate the role of elevated temperature on the nanostructure of films formed both by bi-metallic clusters under deposition and by inert gas condensation followed by compaction.

The paper is organised as follows: Section 2 briefly describes the cohesion model and the Molecular Dynamics

[a] e-mail: mhou@ulb.ac.be

(MD) simulation methods used and the characteristics of the model sample used [11] are briefly described. Section 3 is devoted to a qualitative description of the thermal evolution of model samples at elevated temperature and their diffusive properties. In Section 4, a quantitative method for distinguishing between coalescence and diffusion and determining the diffusion coefficients is presented. The obtained results are discussed. The main conclusions are summarised in Section 5.

2 The simulation model and the model samples

The purpose of this work is to study the thermal evolution of nanostructured samples that were synthesised. The building blocks are Ni_3Al clusters initially modelled as isolated systems containing from a few hundred to a few thousand atoms each [10]. Their thermodynamic equilibrium state in a temperature range from 100 K to 700 K was predicted by Metropolis Monte Carlo modelling (MC) in the semi-grand canonical ensemble [18]. Their assembling at room temperature was then modelled by Molecular Dynamics (MD) with two different models appropriate for modelling the compaction after inert gas condensation and the other for modelling their accumulation by low energy cluster beam deposition [11]. MC simulation starting from the obtained nanostructured model samples allowed finding their new thermodynamic equilibrium state. The study of their thermal evolution at temperatures above 300 K is reported in the present paper.

2.1 The simulation model

A thermal vibration period in a solid is of the order of the picosecond. Since MD allows to study the evolution of a system of the size of our nanostructured samples (twenty to fifty thousand atoms) for times of the order of the nanosecond or more, it is a well suited technique for studying their thermal evolution. Since the two MD techniques employed were already described in previous papers, the models will only be briefly outlined here.

The basic parameter of MD is the interatomic potential describing the interaction between atoms. A many-body potential has been used based on the second moment approximation of the electronic density distribution [19,20] as derived from the tight-binding (TB) theory for transition metals. According to this model, the cohesive energy projected onto one atom can be written as

$$E_i = F(\rho_i) + \frac{1}{2}\sum_{j\neq i}\varphi(r_{ij}) \tag{1}$$

where $F(\rho_i)$ is a function of the electronic density ρ_i at site i and $\varphi(r_{ij})$ is the pairwise contribution of the repulsive energy between atoms i and j separated by the distance r_{ij}. The electronic density ρ_i at the site i is expressed as a functional of pairwise contributions. It may be written as

$$\rho_i = f\left(\sum_{j\neq i}^{N}\Phi(r_{ij})\right). \tag{2}$$

In the second moment TB approximation, this functional is a square root. The total cohesive energy of the system is

$$E_T = \sum_{i=1}^{N} E_i. \tag{3}$$

The functionals φ and F are adjusted semi-empirically and we use the parameterisation in [21–23]. In this expression $\varphi(r_{ij})$ and $\Phi(r_{ij})$ are approximated by a set of cubic splines which parameters are used to fit the potential to the cohesive energy, the equilibrium condition and the elastic constants. A cut-off distance equal to $1.225a_0$, where a_0 is the lattice parameter, limits the range of the local interactions.

In its simplest form, MD merely consists in numerically solving a system of coupled Newton equations of motion in the microcanonical (NVE) statistical ensemble for the particles contained in the simulated box [24,25]. In systems like nanostructured materials, which are characterised by deep inhomogeneities, it is possible to account for the dynamics of the macroscopic anisotropic deformation of the simulation box, at constant external pressure and temperature. This is achieved in the canonical ensemble according to the constrained MD scheme by Rahman and Parrinello (RP-MD) [26,27]. In this scheme, the simulations are performed in the (NPT) ensemble and the system is coupled to a thermal bath by means of the scheme proposed by Nosé [28]. It is not possible to use the RP-MD scheme without further constrains for a system having free surfaces. This is no problem for systems formed by compaction, for which periodic boundary conditions may be applied in three different directions to mimic an infinite system. On the contrary, a nanostructured film formed by cluster beam deposition necessarily has a surface. In addition, it is constrained by the substrate at the interface. Therefore, (NVT) simulations were used in this case. Here, the temperature is also constrained by a thermal bath. The method used however differs from the Nosé scheme in the sense that the Nosé bath is supposed to be the electronic system and the exchange of heat is governed by the electron-phonon coupling (see [13] for further detail). Constant volume is insured by periodic boundary conditions applied to the simulation box and the whole system (including the deposited layer and the substrate upon which it is deposited) is constrained at the same constant temperature.

2.2 The model samples

Free Ni_3Al clusters at thermal equilibrium were prepared by Metropolis Monte Carlo and the method is explained in [10]. It was found that at 700 K and below, isolated equilibrium Ni_3Al clusters containing more than 200 atoms may crystallise and are partitioned into two areas; a core

in the $L1_2$ phase known in bulk materials and a mantle where, depending on the offset of stoechiometry, Al may segregate. In particular, the $L1_2$ phase was found to be stable at the nanoscale as far as the clusters contained 201 atoms or more. Al segregation at the cluster surface was found possible but limited to about 20 percent at room temperature. With such a segregation, the mantle has the fcc structure of a solid solution which coexists with a stable phase in the core. A realistic cluster distribution can be employed for assembling and the cluster sizes were selected small enough to avoid structural effects related to the motion of dislocations. We use a log-normal cluster size distribution and the mean number of atoms per cluster was no more than 7000. The clusters keep their identity and the nanostructure may then be characterised as formed by cluster cores, cluster interfaces and holes. Except some possible local fluctuations in stoechiometry induced by inhomogeneous internal stress, the segregation state of the clusters is similar when they are assembled, whatever the assembling method, or isolated, and the cluster cores keep the stable bulk phase.

In deposition experiments, the slowing down energy of bi-metallic clusters on a metallic surface typically ranges between 0.5 eV/at and 1.5 eV/at. The modelling of deposition is explained in [11,13,16]. The impact may enhance epitaxial accommodation of the cluster, and a competition is found between short and long range ordering, that is, between epitaxy and chemical order. A previous study [29] demonstrated in the case of gold that modelling cluster film formation by classical MD is realistic provided cluster surface diffusion is not involved in the film growth. Cluster assembled materials can also be produced by compaction and the modelling of the Ni_3Al cluster compaction is described in [11]. Similarly to the cluster compacted material, a deposited film displays a complex stacking of nanograins separated by grain boundaries and nanocavities. The grains are however less deformed and the film resembles to a stacking of hard spheres. The volume occupied by cavities is larger and the average density is consequently lower. All cavities are interconnected. No significant correlation between grain orientations and the substrate orientation is found. Only minor epitaxy is found at the interface with Ni and Ni_3Al substrates. None is found with an Al substrate, which is softer. No deposited cluster displays full disorder. The overall chemical disorder is insensitive to the substrate and to the slowing down energy. One common characteristics of the cluster compacted and the cluster deposited nanostructures is that the initially free clusters keep their identity after processing and their cores keep crystalline. They display pronounced chemical and structural order and no pressure or impact induced coalescence is observed. The analysis of pair correlation functions show that significant crystallinity in the grain boundaries is found as well.

The energetics of these model nanostructures is not yet investigated. From the high inhomogeneity of their configurations, they may reasonably be anticipated to display high enthalpy areas that may be responsible for specific thermodynamic behaviours. These represent a class of problems about which experimental and modelling approaches may help to bring substantial understanding. The present work is one step in this direction.

3 Thermal evolution – Qualitative approach

Both model Ni_3Al samples prepared by compaction and by deposition on a Ni(111) surface are at thermal equilibrium at 300 K and zero external pressure. At this temperature, atoms vibrate among their equilibrium position and no significant diffusion is detected over 1 ns simulation, even at the interfaces and internal surfaces. In the present section, a qualitative description of their thermal evolution at higher temperatures is given. A quantitative approach is presented in the next one.

This qualitative approach is based on the examination of atomic configurations. To analyse configurations, it is convenient to distinguish between atoms in grain cores and atoms at surfaces and interfaces. Since grain cores are found to keep their $L1_2$ structure in the temperature range investigated (below the melting temperature of the samples), a convenient parameter to distinguish grain cores from interfacial atoms is the first neighbour coordinance. Atoms in grain cores have a coordinance $Z = 12$ while atoms in interfaces and at surfaces, most generally, have coordinances $Z < 12$ (some are found with $Z = 13$).

Figure 1 compares a slab of a few atomic distances thick in the sample obtained by deposition (Figs. 1a and 1b) and by compaction (Figs. 1c and 1d) at 300 K and after 1 ns isothermal evolution at 700 K. The effect of such a strong increase of temperature is clearly seen to promote contacts between clusters and to reduce the open volumes. The effect is the largest in the sample displaying the largest open volumes. The formation of bottlenecks can be observed, which is typical to coalescence. In Figure 1b, the interface with the substrate is not as spectacularly modified, suggesting that the substrate is not playing a major role in the thermal evolution of the film.

The fraction of miscoordinated atoms (with $Z \neq 12$) was measured as a function of time for both samples and the results are given in Figure 2 for the deposited film. The figure shows this fraction to decrease with time. It however decreases by no more than 10 percent in 1 ns. This decrease is an additional evidence for coalescence or sintering. This evolution, shown on the example of the deposited sample, is slower in the case of the compacted sample, which is also the densest one at 300 K. Since open volumes are smaller, it displays a better resistance to a heat treatment, although its evolution at high temperature is found qualitatively similar (Figs. 1c and 1d). The mean square thermal displacement (denoted by Δ^2 in what follows) was determined in both samples as a function of time at several temperatures between 300 K and 800 K. The results at 700 K are displayed in Figure 3. Δ^2 is shown for all particles as well as, distinctly, for atoms with $Z \neq 12$ (Δ_1^2) and $Z = 12$ (Δ_2^2). For those atoms which coordinance changes with time, the contributions to Δ_1^2 and Δ_2^2 are distinguished. The time dependencies in cluster cores and interfaces are clearly different and the dependency for

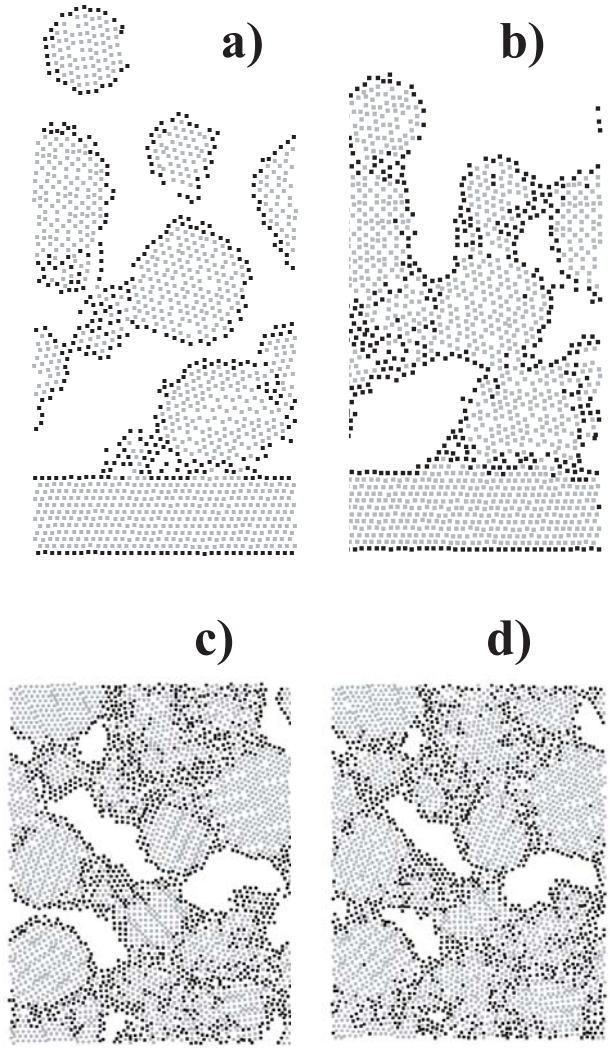

Fig. 1. Slabs in Ni_3Al nanostructured samples; (a) deposited sample at equilibrium at 300 K, (b) the same slab as in (a), after thermal evolution at 700 K during one nanosecond, (c) Slab in the compacted sample at equilibrium at 300 K, (d) the same slab as in (c), after thermal evolution at 700 K during one nanosecond.

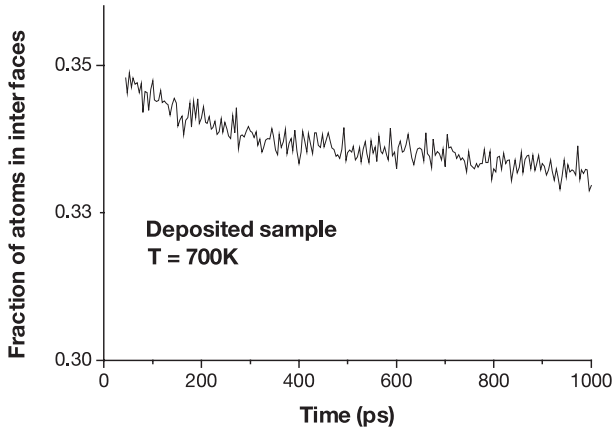

Fig. 2. Time dependence of the fraction of atoms at internal surfaces and interfaces during the time evolution of the deposited film at 700 K.

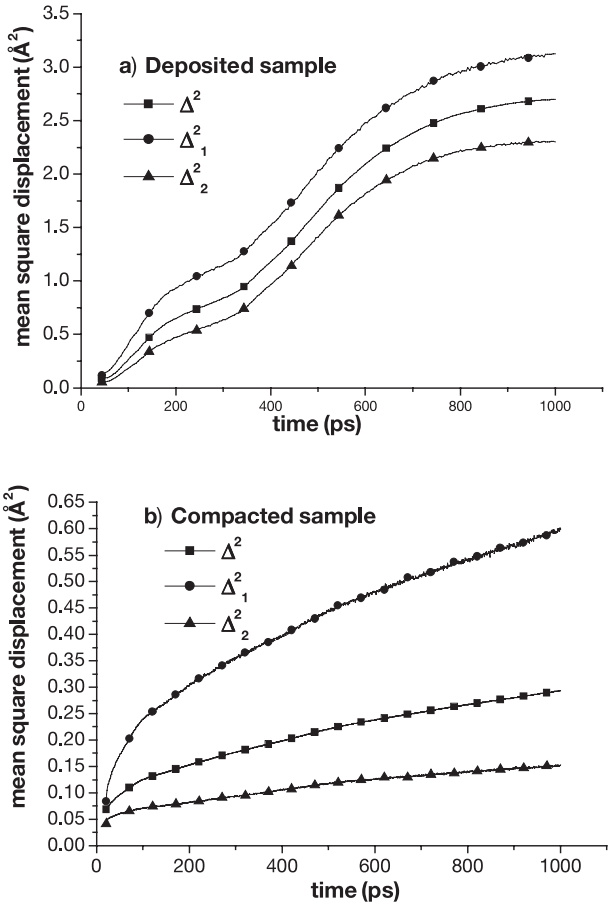

Fig. 3. Mean square displacements of atoms (a) in the deposited sample, (b) in the compacted sample. Results are displayed for all atoms (Δ^2), atoms at internal surfaces and interfaces (Δ_1^2) and atoms in grain cores (Δ_2^2).

all particles is a convolution of both. The results for the compacted sample (Fig. 3b) are similar to what may be expected for pure atomic diffusion, but this is also the sample where less coalescence and cluster motion are observed. The configurations indicate that, at 700 K, core atoms still form an equilibrium crystal structure. Hence, the essential of the thermal evolution is characterised by the diffusion of interfacial and surface atoms on the one hand, and the motion of each core as a whole on the other. Coalescence and atomic diffusion proceed simultaneously and the results in Figure 2 are the consequence of both. The distinction between both processes is however necessary for a better quantitative analysis, and this distinction is made in the next section.

4 Thermal evolution – Quantitative approach

The starting point is the mean square displacement of the atoms of the samples at different temperatures, as calculated in the previous section, in which one distinguishes between the diffusional motion of individual atoms and the motion of clusters as a whole. To this purpose, the time evolution of the sample is expressed in terms of a

rigid body motion of individual clusters and the diffusion of atoms at the surface and the interfaces. A simple model helps to distinguish between these motions and thus to determine the diffusion coefficient of atoms at the surface of the clusters. Advantage is taken from the fact that the decrease of the number of interfacial atoms is slow as compared to the time needed to measure a diffusion coefficient.

In what follows, the total displacement of each atom is represented as the sum of a collective and a diffusive component. Let $\mathbf{r}_i^0$ be the displacement of the ith atom due to the collective motion of all atoms in the cluster to which it belongs. Let $\mathbf{r}_i^1$ be the displacement of the same atom due to thermal diffusion at a cluster interface and $\mathbf{r}_i^T$ its displacement due to thermal vibration among an equilibrium position. Then, the position of this atom may be written as follow:

$$\mathbf{r}_i(t) = \mathbf{r}_i(0) + \mathbf{r}_i^0(t) + \mathbf{r}_i^1(t) + \mathbf{r}_i^T(t). \tag{4}$$

In the next, the following notation is used. $\sum'$ is the sum over atoms with $Z \neq 12$ and $\sum''$ is the sum over those with $Z = 12$, N_1 is the number of atoms with $Z \neq 12$ and N_2 the number of atoms with $Z = 12$. $N = N_1 + N_2$ is the total number of atoms in the simulation box. Using these notations, the mean square displacement for all atoms in the box and for the atoms at the interface and in the core of the clusters may be expressed as

$$\begin{aligned}
\Delta^2 &= \frac{1}{N}\sum_i \left[\frac{1}{t}\int \mathbf{r}_i^2\,\mathrm{d}t - \left(\frac{1}{t}\int \mathbf{r}_i\,\mathrm{d}t\right)^2\right] \\
\Delta_1^2 &= \frac{1}{N_1}\sum_i{}' \left[\frac{1}{t}\int \mathbf{r}_i^2\,\mathrm{d}t - \left(\frac{1}{t}\int \mathbf{r}_i\,\mathrm{d}t\right)^2\right] \\
\Delta_2^2 &= \frac{1}{N_2}\sum_i{}'' \left[\frac{1}{t}\int \mathbf{r}_i^2\,\mathrm{d}t - \left(\frac{1}{t}\int \mathbf{r}_i\,\mathrm{d}t\right)^2\right].
\end{aligned} \tag{5}$$

In principle, in order to account for the coordinance fluctuations with time, it is necessary, in the calculations of the mean values in equations (5), to integrate only over those periods of time where the atoms belong to the corresponding group. However, since the decrease of non-perfectly coordinated atoms only decrease by 10 percent over the nanosecond used to evaluate equations (5), N_1 and N_2 are approximated to be time independent.

With this approximation, using (5), we can get

$$\begin{aligned}
\Delta^2 &= \frac{1}{N}\sum_i \varphi_i(t) + N_1/(N_1+N_2)Dt + \Delta_T^2 \\
\Delta_1^2 &= \frac{1}{N_1}\sum_i{}' \varphi_i'(t) + Dt + \Delta_{1T}^2 \\
\Delta_2^2 &= \frac{1}{N_2}\sum_i{}'' \varphi_i''(t) + \Delta_{2T}^2
\end{aligned} \tag{6}$$

$$\varphi_i = \left[\frac{1}{t}\int \mathbf{r}_i^{0^2}\,\mathrm{d}t - \left(\frac{1}{t}\int \mathbf{r}_i^0\,\mathrm{d}t\right)^2\right], \tag{7}$$

D is the diffusion coefficient of the atoms at the interfaces.

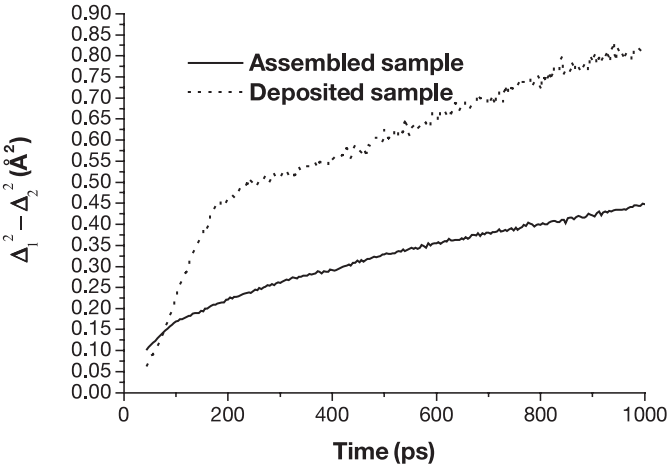

Fig. 4. Difference $\Delta_1^2 - \Delta_2^2$ as a function of time for both samples at 700 K, illustrating how the diffusive component is extracted from the time dependence of the mean square atomic displacement.

From (7) we can see that in order to determine the diffusion coefficient it is necessary to find the linear part of Δ^2, if any. We can do this if we compare the expressions for Δ_1^2 and Δ_2^2. The non-linear part in these expressions is due to the collective component of the clusters motion. If one considers that every atom have the same contribution to collective motion, namely that $\varphi_i = \varphi_k$ for all i and k, they also have equal contributions to the sums $\sum'$ and $\sum''$ and these sums are proportional to the numbers of particles N_1 and N_2 respectively. Then, one can write

$$\frac{1}{N_1}\sum_i{}' \varphi_i'(t) = \frac{1}{N_2}\sum_i{}'' \varphi_i''(t). \tag{8}$$

Using (6) and (8), the diffusion coefficient is deduced from the difference $\Delta_1^2 - \Delta_2^2$. This difference is represented in Figure 4 as a function of time for both samples at 700 K. It is representative of the temperature range considered (400–800 K). After about 200 ps during which collective and diffusive motions are hardly distinguished, the time dependencies get linear and the present method becomes valid. Indeed, the diffusive contribution to the mean square displacement is extracted and the calculation of diffusion coefficients can be done. In Figure 5 the temperature dependence of the diffusion coefficient deduced from Figure 4 is presented for both samples. It is well described by an Arrhenius law. Pre-factors and activation energies can be deduced. One finds $D_0 = 6.3\times10^{-10}$ m^2/s, $E_a = 0.3$ eV and $D_0 = 9.3 \times 10^{-10}$ m^2/s, $E_a = 0.3$ eV for the cluster deposited and compacted nanostructured samples respectively. The pre-factors are comparable and activation energies are the same.

This activation energy is quite low as compared to other known or model systems where no correlated motion take place. For instance, we estimated the surface diffusion coefficient at different temperatures on a solid Ni_3Al surface with a saw tooth rough structure with the same characteristic length as the mean cluster diameter

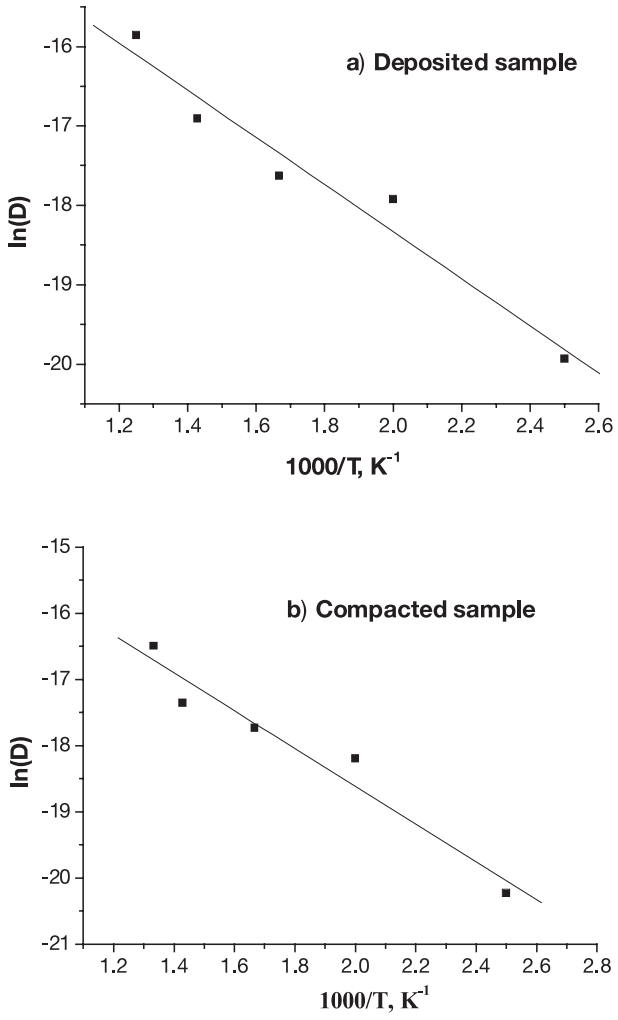

Fig. 5. Temperature dependence of the diffusion coefficient in the form of Arrhenius plots (a) for the deposited sample and (b) for the assembled sample.

in the nanostructured samples. Periodical boundary conditions were applied in two orthogonal directions parallel to the mean rough plane orientation. A pre-factor $D_0 = 3.4\times10^{-10}$ m^2/s, and an activation energy $E_a = 0.4$ eV are found in the same temperature range as for the nanostructured samples. The activation energy is somewhat higher. This probably reflects the effect of the higher symmetry of this surface as compared to the internal surfaces and interfaces of the nanostructured samples. We also estimated the diffusion coefficient for adatoms on planar surfaces and in liquid Ni_3Al. Activation energies $E_a = 0.6$ eV and $E_a = 0.3$ eV for adatoms and the liquid respectively. Hence, the activation energy for thermal diffusion in the solid nanostructured samples has the same value as in the liquid phase. This suggests that, at the elevated temperatures considered, internal surfaces and interfaces behave as liquids coexisting with solid grain cores, which is consistent with the observation of bottlenecks and coalescence in Figure 1.

5 Summary

The diffusive properties of Ni_3Al nanostructured materials were investigated. Two different model samples were used therefore. One was prepared by low energy cluster beam deposition and the other by cluster compaction. Both are at thermal equilibrium at 300 K and zero external pressure. Comparison between configurations of the films at 300 K and after 1 ns heating at 700 K revealed remarkable differences between them. When heating at 700 K, the grain cores remain crystalline but the volume of the pores between individual clusters becomes smaller. Bottlenecks formation is observed between individual clusters, which is an indication for coalescence. The compacted sample, which is also the densest one at 300 K, displays a better resistance to a heat treatment, although its evolution was found qualitatively similar.

To evaluate particle diffusion along the surface of the clusters, the time dependence of the mean square displacement of the atoms was examined at different temperatures. It was calculated distinctly for the atoms at the clusters surfaces and interfaces and for those in the cluster cores. On the basis of these calculations it was found that the diffusion coefficient for interfacial and surface atoms obey an Arrhenius law with an activation energy of 0.3 eV, which is the same as estimated for the liquid phase. This is an indication for the coexistence of a the liquid interfacial layer with solid grain cluster cores.

One of us (PM) is grateful to the Federal Belgian Government for a grant for taking part in the present research program at the Université Libre de Bruxelles. This work is achieved within the co-operation agreement IAP 5-1 with the Federal Belgian Government.

References

1. K. Lu, H.Y. Zhang, J. Fecht, J. Mat. Res. **12**, 9223 (1997)
2. S.R. Philipot, D. Wolf, H. Gleiter, J. Appl. Phys. **78**, 845 (1995)
3. J. Wang, D. Wolf, S.R. Phillpot, Philos. Mag. A **73**, 517 (1996)
4. H. van Swygenhoven, A. Caro, Appl. Phys. Lett. **71**, 1652 (1997)
5. H. van Swygenhoven, A. Caro, Phys. Rev. **58**, 11246 (1998)
6. H. van Swygenhoven, M. Spaczer, D. Farkas, A. Caro, Nanostr. Mat. **12**, 323 (1999)
7. P. Keblinski, D. Wolf, S.R. Phillpot, H. Gleiter, Scr. Mater. **41**, 631 (1999)
8. A. Caro, H. van Swygenhoven, Phys. Rev. B **63**, 134101 (2001)
9. R. Peyer, S. Prakash, P. Entel, Phase Transitions **75**, 51 (2002)
10. E.E. Zhurkin, M. Hou, J. Phys. C **12**, 6735 (2000)
11. M. Hou, V. Kharlamov, E.E. Zhurkin, Phys. Rev. B **66**, 195408 (2002)
12. H. Haberland, Z. Insepov, M. Moseler, Phys. Rev. B **51**, 11061 (1995)
13. Q. Hou, M. Hou, L. Bardotti, B. Prével, P. Mélinon, A. Perez, Phys. Rev. B **62**, 2825 (2000)

14. H. Hsieh, R.S. Averback, H. Flynn, Phys. Rev. B **45**, 4417 (1992)
15. V.S. Kharlamov, E.E. Zhurkin, M. Hou, Nucl. Instr. Meth. B **193**, 538 (2002)
16. M. Hou, Nucl. Instr. Meth. B **135**, 501 (1998)
17. Y. Ashkenazy, R.S. Averback, K. Albe, Phys. Rev. B **64**, 205409 (2001)
18. S.M. Foiles, Phys. Rev. B **32**, 7685 (1985)
19. F. Ducastelle, J. Phys. **31**, 133 (1970)
20. M.W. Finnis, J.E. Synclair, Phil. Mag. A **50**, 45 (1984)
21. G.J. Ackland, V. Vitek, Mat. Res. Soc. Symp. Proc. **133**, 105 (1989)
22. G.J. Ackland, V. Vitek, Phys. Rev. B **41**, 10324 (1990)
23. F. Gao, D. Bacon, G. Ackland, Phil. Mag. A **67**, 275 (1993)
24. M.P. Allen, D. Tildesley, *Computer Simulation of Liquid* (Clarendon Press, Oxford, 1987)
25. D. Frenkel, B. Smit, *Understanding Molecular Simulation: From Algorithms to Applications* (Academic Press, San Diego-London-Boston-New York-Tokyo-Toronto, 1996)
26. M. Parrinello, A. Rahman, Phys. Rev. Lett. **45**, 1196 (1980)
27. M. Parrinello, A. Rahman, J. Appl. Phys. **52**, 7182 (1981)
28. S. Nosé, J. Chem. Phys. **81**, 511 (1984)
29. L. Bardotti, B. Prével, P. Mélinon, A. Perez, Q. Hou, M. Hou, Phys. Rev. B **62**, 2835 (2000)